Study on Electromagnetic Force and Vibration of Turbogenerator End Windings under Impact Load(Ⅰ):

Analysis of Electromagnetic Force of End Windings under Impact Load

Huang Xueliang[*]　　　Hu Minqiang

(Department of Electrical Engineering, Southeast University, Nanjing 210096, China)

Abstract:　In this paper, the boundary value problem (BVP) of 3-D transient eddy current field in the end region in the case that the generator is affected by impact load is specified. Besides, ways to implement discrete methods in both time domain and space domain during the solution of the problem are investigated. The Crank-Nicolson scheme is utilized to attain the iterative format of time differential, after taking factors that can ensure both computation precision and stability into consideration. In this paper, the magnetic distribution in the end region of a turbogenerator in the case that the generator is affected by impact load is specified. As a result, it provides foundation for further study of electromagnetic force and electromagnetic vibration in the end region of the turbogenerator.

Key words:　turbogenerator, transient eddy current field, impact load, electromagnetic force, electromagnetic vibration

Presently, with the growing number of large-scale and super-scale corporations (i.e., large-scale steel corporations and chemical plants), the structure of power distribution has changed greatly. Because some high-power devices in these corporations and plants may start frequently, which lead to frequent short-time impact load and, as a result, hidden trouble to the secure operation of electric network and generators. In particular, when the impact load occurs in such positions that are very near to a power plant, the generator set in this plant will be impacted greatly. Because the impact load in this case may lead to violent fluctuations of the stator current, active power and reactive power of the generator. Then, tremendous electromagnetic force is produced in the end region of the generator. As a result, winding fault is possible. Besides, electromagnetic vibration in the end region of the generator caused by frequent impact loads speeds up the wear and tear of the conductor insulation coat, which can make up the reason of flexible winding structure and lead to more dramatic vibration of the winding. Therefore, it's important to carry out the study on the electromagnetic force distribution and electromagnetic vibration in the end region of the turbogenerator in various working conditions.

1　Analysis of the 3-D Transient Eddy Current Field in the End Region in the Case That the Generator Is Affected by Impact Load

The boundary value problem of 3-D transient eddy current field in the end region can be expressed as follows[1]:

$$\left.\begin{array}{ll} \nabla \times \nu \nabla \times \boldsymbol{A} + \sigma \dfrac{\partial \boldsymbol{A}}{\partial t} = \boldsymbol{J}_{\mathrm{S}} & \forall P \in V \\[2mm] \boldsymbol{A} = \boldsymbol{A}_0 & \forall P \in S_1 \\[2mm] \boldsymbol{n} \times (\nabla \times \boldsymbol{A}) = -\mu \boldsymbol{\delta}_{\mathrm{S}} & \forall P \in S_2 \end{array}\right\} \tag{1}$$

where $\boldsymbol{A}$ is the vector magnetic potential; $\boldsymbol{J}_{\mathrm{S}}$ is the current density of the conductor; $\boldsymbol{\delta}_{\mathrm{S}}$ is the area current density in the boundary; $\boldsymbol{n}$ is the vertical direction; ν, σ, μ are the magnetic reluctivity, electric conductivity and magnetic conductivity of the medium respectively; P is an arbitrary point inside the solving domain; V is the solving domain; S_1 denotes the Dirichlet problem and S_2 denotes the Neumann problem.

If the transient eddy current field is assumed to be a temporally steady-state one before the point $t = 0$ and the point itself, the field distribution $\boldsymbol{A}(t_0)$ at the point $t = 0$ can be specified in the same way as resolving steady-state eddy current field. In other words, $\boldsymbol{A}(t_0)$ must meet the demands of the following equations[2]

$$
\left.\begin{array}{ll}
\nabla \times \nu \nabla \times \boldsymbol{A}(t_0) + \mathrm{j}\omega\sigma\boldsymbol{A}(t_0) = \boldsymbol{J}_\mathrm{S}(t_0) & \forall P \in V \\
\boldsymbol{A}(t_0) = \boldsymbol{A}_0(t_0) & \forall P \in S_1 \\
\boldsymbol{n} \times (\nabla \times \boldsymbol{A}(t_0)) = -\mu\boldsymbol{\delta}_\mathrm{S}(t_0) & \forall P \in S_2
\end{array}\right\} \tag{2}
$$

where ω is the angular speed.

For convenience, the vector magnetic potential $\boldsymbol{A}$, the body current density $\boldsymbol{J}_\mathrm{S}$ and the area current density $\boldsymbol{\delta}_\mathrm{S}$ are supposed and expressed in a cylindrical coordinate as follows:

$$
\left.\begin{array}{l}
\boldsymbol{A} = [A_r(r,z,t)\boldsymbol{e}_r + \mathrm{j}A_\theta(r,z,t)\boldsymbol{e}_\theta + A_z(r,z,t)\boldsymbol{e}_z]\,\mathrm{e}^{\mathrm{j}p\theta} \\
\boldsymbol{J}_\mathrm{S} = [J_{r\mathrm{S}}(r,z,t)\boldsymbol{e}_r + J_{\theta\mathrm{S}}(r,z,t)\boldsymbol{e}_\theta + J_{z\mathrm{S}}(r,z,t)\boldsymbol{e}_z]\,\mathrm{e}^{\mathrm{j}p\theta} \\
\boldsymbol{\delta}_\mathrm{S} = [\delta_{r\mathrm{S}}(r,z,t)\boldsymbol{e}_r + \delta_{\theta\mathrm{S}}(r,z,t)\boldsymbol{e}_\theta + \delta_{z\mathrm{S}}(r,z,t)\boldsymbol{e}_z]\,\mathrm{e}^{\mathrm{j}p\theta}
\end{array}\right\} \tag{3}
$$

where P is the number of pole-pairs of the electric machine; $\boldsymbol{e}_r$, $\boldsymbol{e}_\theta$, $\boldsymbol{e}_z$ denote the direction of r, θ, z respectively.

Weighted integration is carried out in both sides of Eq.(1) by choosing appropriate weight function $\boldsymbol{W}$ of the vector.

$$
\int_V \boldsymbol{W} \cdot \nabla \times (\nu \nabla \times \boldsymbol{A})\,\mathrm{d}V + \int_V \boldsymbol{W} \cdot \sigma \frac{\partial \boldsymbol{A}}{\partial t}\,\mathrm{d}V = \int_V \boldsymbol{W} \cdot \boldsymbol{J}_\mathrm{S}\,\mathrm{d}V \tag{4}
$$

Eq.(4) can be expressed as

$$
\int_V (\nabla \times \boldsymbol{W}) \cdot (\nu \nabla \times \boldsymbol{A})\,\mathrm{d}V + \int_V \boldsymbol{W} \cdot \sigma \frac{\partial \boldsymbol{A}}{\partial t}\,\mathrm{d}V = \int_V \boldsymbol{W} \cdot \boldsymbol{J}_\mathrm{S}\,\mathrm{d}V + \oint_S [\boldsymbol{W} \times (\nu \nabla \times \boldsymbol{A})] \cdot \boldsymbol{n}\,\mathrm{d}S \tag{5}
$$

According to the Galinkin law, the weighted function is chosen as follows:

$$
\boldsymbol{W} = (N\boldsymbol{e}_r + \mathrm{j}N\boldsymbol{e}_\theta + N\boldsymbol{e}_z)\mathrm{e}^{\mathrm{j}p\theta}
$$

where N is the form function of the element, whose expression have been written in Refs.[1 – 4].

The first integration item on the left side of Eq.(5) can be evaluated from the curl expressions of the vector magnetic potential and weighted function in the cylindrical coordinate

$$
f_1 = \int_{Ve} \sum_{j=1}^3
\begin{bmatrix}
\nu_\theta \dfrac{\partial N_j}{\partial z}\dfrac{\partial N_i}{\partial z} - \nu_z \dfrac{p^2}{r^2}N_jN_i & \nu_z \dfrac{1}{r^2}\dfrac{\partial N_j}{\partial r}N_i & -\nu_\theta \dfrac{\partial N_j}{\partial r}\dfrac{\partial N_i}{\partial z} \\[2ex]
\nu_z \dfrac{p}{r^2}N_jN_i + \nu_z \dfrac{p}{r^2}N_j\dfrac{\partial N_i}{\partial r} & -\nu_r \dfrac{\partial N_j}{\partial z}\dfrac{\partial N_i}{\partial z} - \nu_z \dfrac{1}{r^2}\Big(N_j + r\dfrac{\partial N_j}{\partial r}\Big)\Big(N_i + r\dfrac{\partial N_i}{\partial r}\Big) & \nu_r \dfrac{p}{r}N_j\dfrac{\partial N_i}{\partial z} \\[2ex]
-\nu_\theta \dfrac{\partial N_j}{\partial z}\dfrac{\partial N_i}{\partial r} & \nu_r \dfrac{p}{r}\dfrac{\partial N_j}{\partial z}N_i & -\nu_r \dfrac{p^2}{r^2}N_jN_i + \nu_\theta \dfrac{\partial N_j}{\partial r}\dfrac{\partial N_i}{\partial r}
\end{bmatrix}
\begin{bmatrix} A_{rj} \\ A_{\theta j} \\ A_{zj} \end{bmatrix}\mathrm{e}^{2\mathrm{j}p\theta}\,\mathrm{d}V \tag{6}
$$

where N_i, N_j denote the form function of the node i, j.

The second integration item in the left side of Eq.(5) is

$$
f_2 = \int_{Ve} \sum_{j=1}^3 N_iN_j\sigma
\begin{bmatrix} \dfrac{\partial A_{rj}}{\partial t} \\[1.5ex] -\dfrac{\partial A_{\theta j}}{\partial t} \\[1.5ex] \dfrac{\partial A_{zj}}{\partial t} \end{bmatrix}
\mathrm{e}^{2\mathrm{j}p\theta}\,\mathrm{d}V \tag{7}
$$

The first integration item in the right side of Eq.(5) is

$$
p_1 = \int_{Ve} N_i
\begin{bmatrix} J_{r\mathrm{S}} \\ -J_{\theta\mathrm{S}} \\ J_{z\mathrm{S}} \end{bmatrix}
\mathrm{e}^{2\mathrm{j}p\theta}\,\mathrm{d}V \tag{8}
$$

The second integration item in the right side of Eq.(5) is

$$
p_2 = \oint_S [\boldsymbol{N}_i \times (\nu \nabla \times \boldsymbol{A})] \cdot \boldsymbol{n}\,\mathrm{d}S = \oint_S N_i
\begin{bmatrix} \delta_{r\mathrm{S}} \\ -\delta_{\theta\mathrm{S}} \\ \delta_{z\mathrm{S}} \end{bmatrix}
\mathrm{e}^{2\mathrm{j}p\theta}\,\mathrm{d}S \tag{9}
$$

In each integration items of Eq.(5), the integral result of it is a constant, which can be neglected during the computation without affecting the validity of the equation. Substitute Eqs.(6) – (9) into (5), the expression of the computation matrix of the element can be attained.

$$
\boldsymbol{K}_\mathrm{e}\boldsymbol{A}_\mathrm{e} + \boldsymbol{K}_{t_\mathrm{e}} \frac{\partial \boldsymbol{A}_\mathrm{e}}{\partial t} = \boldsymbol{P}_\mathrm{e} \tag{10}
$$

where e denotes element. The right side of Eq.(10) is

$$\boldsymbol{P}_e = \begin{bmatrix} p_1 \\ p_2 \\ p_3 \end{bmatrix} = \begin{bmatrix} \iint\limits_{Se} J_{rS} N_i r \mathrm{d}r\mathrm{d}z \\ \iint\limits_{Se} - J_{\theta S} N_i r \mathrm{d}r\mathrm{d}z \\ \iint\limits_{Se} J_{zS} N_i r \mathrm{d}r\mathrm{d}z \end{bmatrix} \tag{11}$$

The coefficient matrix can be expressed as

$$\boldsymbol{K}_e = \begin{bmatrix} k_{11} & k_{12} & k_{13} \\ k_{21} & k_{22} & k_{23} \\ k_{31} & k_{32} & k_{33} \end{bmatrix} \tag{12}$$

$$\boldsymbol{K}_{t_e} = \begin{bmatrix} k_t & & \\ & - k_t & \\ & & k_t \end{bmatrix} \tag{13}$$

With the introduction of Crank-Nicolson method[5,6], Eq.(10) can be expressed as

$$\left[\frac{\boldsymbol{K}_e}{2} + \frac{\boldsymbol{K}_{t_e}}{\Delta t} \right] A_e^n = \left[- \frac{\boldsymbol{K}_e}{2} + \frac{\boldsymbol{K}_{t_e}}{\Delta t} \right] A_e^{n-1} + \frac{\boldsymbol{P}_e^n + \boldsymbol{P}_e^{n-1}}{2} \tag{14}$$

Eq.(14) is the computation matrix expression of the element when substituting the derivative item with the forward first order difference of A to time variable, and introducing the Crank-Nicolson method. Where A_e^{n-1} and A_e^n are values of the vector magnetic potentials at t_{n-1} and t_n respectively, $\boldsymbol{K}_e$ and $\boldsymbol{K}_{t_e}$ are shown in Eqs.(12) and (13) respectively. While $\boldsymbol{P}_e^n$ and $\boldsymbol{P}_e^{n-1}$ denote items in the right side at t_n and t_{n-1} excited by current respectively.

2 Computation of the Electromagnetic Force in End Region under Impact Load

The Lorentz force of the conductor element in magnetic field is $\mathrm{d}\boldsymbol{F}_l = I\mathrm{d}L \times \boldsymbol{B}$. As a result, when current I flows through conductor element $\mathrm{d}\boldsymbol{L}$ in magnetic field, the Lorentz force density $\boldsymbol{f}$ can be expressed as

$$\boldsymbol{f} = \boldsymbol{I} \times \boldsymbol{B} \tag{15}$$

where $\boldsymbol{I}$ is the current that flows through the conductor, whose direction accords with that of the conductor element; and $\boldsymbol{B}$ is the flux density at the conductor element.

In cylindrical coordinate, Eq.(15) can be expressed as

$$f = (i_\theta B_z - i_z B_\theta)e_r + (i_z B_r - i_r B_z)e_\theta + (i_r B_\theta - i_\theta B_r)e_z \tag{16}$$

In the process of computation, end winding of the stator is divided into many segments first. Then, the flux density of each segment can be attained according to the spacial magnetic distribution at moment t. After that, the force density distribution of the end winding can be attained according to current of the winding at this moment. Finally, the magnetic force of the end winding at moment t can be attained by numerical integration method.

3 Computation Examples

Taking the No.2 generator of Huaneng Plant (Nanjing) (As shown in Fig.1, made in Russia (former USSR), capacity:320 MW, type:TBB-320-2EY3) for example, the transient magnetic field and electromagnetic force in end region under impact load are calculated.

The external activation in the process of calculation comes from field measurement data. Fig.2 and Fig.3 show the oscillograms of three-phase current and voltage of the stator under impact load (These marked data indicate field measurement data.). The values of the current and voltage in these figures are ratios of practical values to basal values.

The transient distribution of the electromagnetic field in the end region of the generator is calculated. Fig.4 shows the flux density distribution in the case $t = 24.280\,0$ s, $t = 24.282\,5$ s, $t = 24.285\,0$ s, $t = 24.287\,5$ s and $t = 24.290\,0$ s. From the flux density distribution in
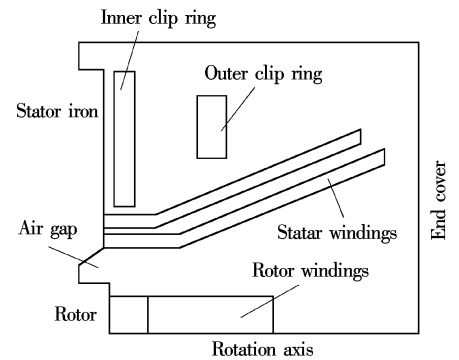

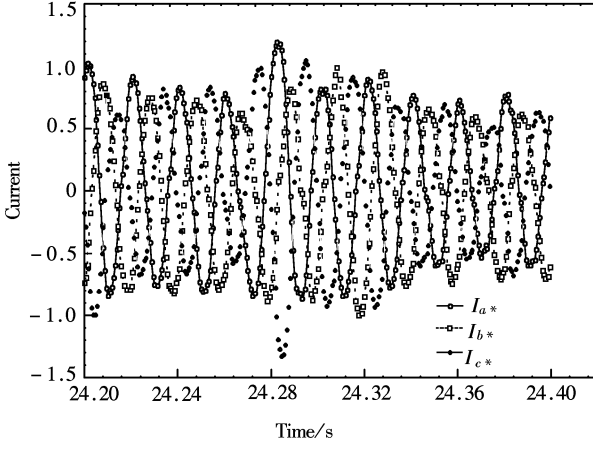Fig.1 Structural diagram of turbogenerator end region

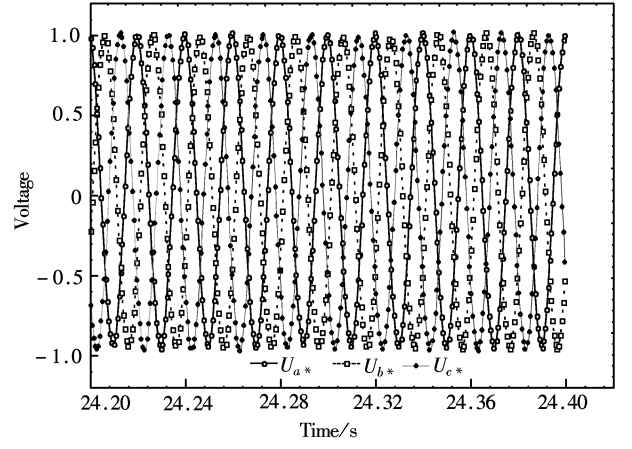Fig.2   Three-phase current of stator under impact load moment

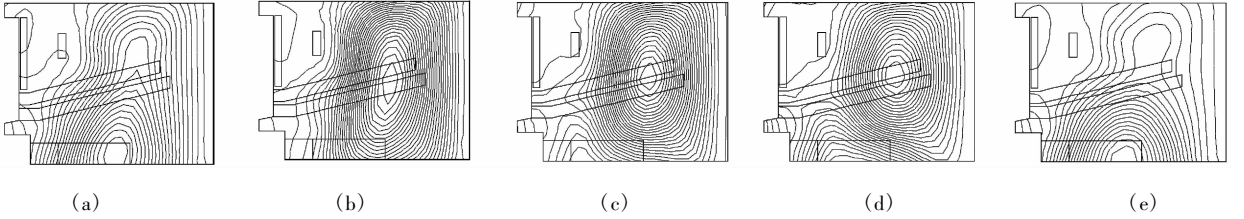Fig.3   Three-phase voltage of stator under impact load

(a)   (b)   (c)   (d)   (e)

Fig.4   Magnetic figure of the end region. (a) $t = 24.280\,0$ s; (b) $t = 24.282\,5$ s; (c) $t = 24.285\,0$ s; (d) $t = 24.287\,5$ s; (e) $t = 24.290\,0$ s

the end region, it can be learned that the flux densities in end structures are decreased because of the eddy current in the clamping ring, which leads to decreased iron loss in the end region.

Fig.5 shows the way that magnetic flux density changes with time when impact load occurs.

Fig.6 shows the electromagnetic force distribution in the end winding at the moment $t = 24.280\,0$ s, $t = 24.282\,5$ s, $t = 24.285\,0$ s, $t = 24.287\,5$ s and $t = 24.290\,0$ s.

From the above figures, it can be learned that electromagnetic force in the end winding within a half power period ranging from $t = 28.28$ s to $t = 28.29$ s changes periodically with time. This reflects the effect of electromagnetic potential rotation on electromagnetic force of the winding.
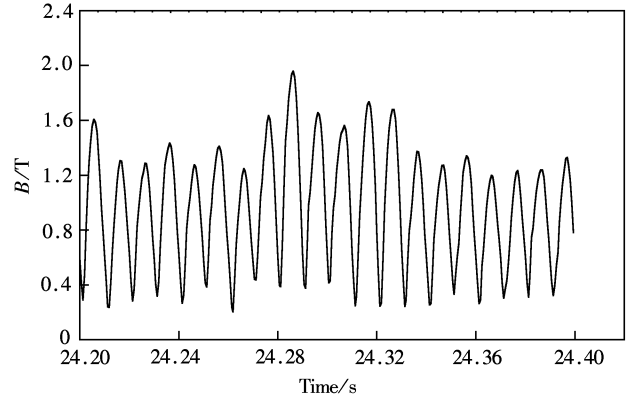

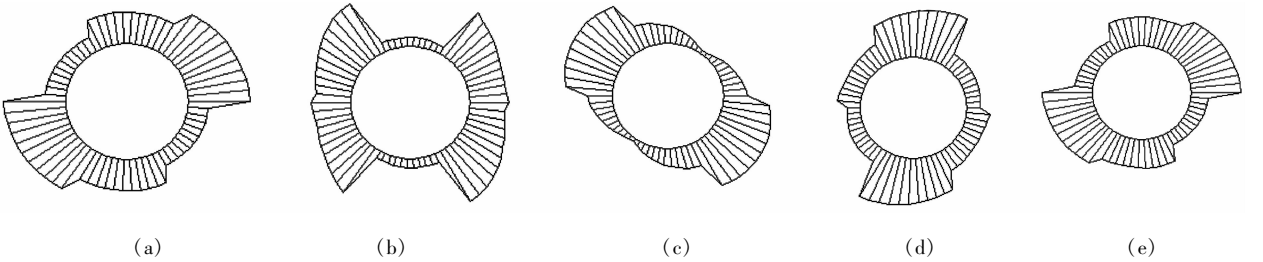**Fig**.5   The way that magnetic flux density changes with time at a point in air gap

(a)   (b)   (c)   (d)   (e)

Fig.6   The electromagnetic force distribution in the end winding at the moment (a) $t = 24.280\,0$ s; (b) $t = 24.282\,5$ s; (c) $t = 24.285\,0$ s; (d) $t = 24.287\,5$ s; (e) $t = 24.290\,0$ s

4   Conclusion

In this paper, a mathematical model of the distribution of 3-D transient eddy current field in the end region is established. And the algorithm that can ensure both precision and stability during the calculation is specified.

When impact load occurs, the terminal voltage of the generator doesn't change much, while the current changes dramatically. As a result, corresponding windings bears the impact of abnormal electromagnetic force. The calculation of the transient electromagnetic field distribution in the end region and electromagnetic force density distribution of the winding under impact load will provide foundation for further study of electromagnetic force and electromagnetic vibration in the end region of the turbogenerator.

References

［1］ Zhou Keding. *Numerical calculation theory and application of engineering electromagnetic field*［M］. Beijing：High Education Press, 1994.（in Chinese）

［2］ Huang Xueliang. Research on the eddy current electromagnetic field in the end region of turbogenerator and on factors which affects the field［J］. *Transactions of China Electrotechnical Society*, 1996, **11**(2):1－6.（in Chinese）

［3］ Lavers J D. Electromagnetic field computation in power engineering［J］. *IEEE Trans on MAG*, 1993, **29**(6):2347－2352.

［4］ Zhou E. Solution of 3D eddy current electromagnetic fields and losses in the end region of turbogenerator［A］. In：Chen Yongxiao ed. *Proceedings of the 2nd Chinese International Conference on Electrical Machines*［C］. Beijing：International Academic Press, 1995.674－677.

［5］ Hu Minqiang. Analysis of the complex variational problem of low frequency electromagnetic field［J］. *Transactions of China Electrotechnical Society*, 1998, **13**(3):27－29.（in Chinese）

［6］ Celozz1 S, Feliziani M. Time domain finite element simulation of conductive regions［J］. *IEEE Trans on MAG*, 1993, **29**(2):1705－1710.

冲击负荷下汽轮发电机端部绕组电动力及其振动问题的研究(Ⅰ):端部绕组电动力分析

黄学良　　胡敏强

（东南大学电气工程系,南京 210096）

摘　要　本文给出了冲击负荷下发电机端部三维瞬态涡流场的边值问题,并阐述了求解该问题时在空间、时间上的离散方法.在综合考虑计算精度和计算稳定性两方面因素的基础上,运用 Crank-Nicolson 方法得到了时间差分的迭代格式.在此基础上,详细分析了冲击负荷下汽轮发电机的端部电磁场.本文的研究为进一步分析发电机端部绕组电动力及电磁振动提供了依据.

关键词　汽轮发电机,瞬态涡流场,冲击负荷,电动力,电磁振动

中图分类号　TM311